


Development and characterization of lanolin incorporated electrospun nanofibers for nursing pads

C. Akduman, E. P. Akcakoca Kumbasar & I. Ozguney


To cite this article: C. Akduman, E. P. Akcakoca Kumbasar & I. Ozguney (2022): Development and characterization of lanolin incorporated electrospun nanofibers for nursing pads, The Journal of The Textile Institute, DOI: [10.1080/00405000.2022.2145442](https://doi.org/10.1080/00405000.2022.2145442)

To link to this article: <https://doi.org/10.1080/00405000.2022.2145442>

 View supplementary material 

 Published online: 14 Nov 2022.



 Submit your article to this journal 

 Article views: 139

 View related articles 

 View Crossmark data 

Development and characterization of lanolin incorporated electrospun nanofibers for nursing pads

C. Akduman^a , E. P. Akcakoca Kumbasar^b  and I. Ozgüney^c 

^aDepartment of Textile Technology, Denizli Vocational School of Technical Sciences, Pamukkale University, Denizli, Turkey; ^bTextile Engineering, Ege University, Izmir, Turkey; ^cDepartment of Pharmaceutical Technology, Faculty of Pharmacy, Ege University, Izmir, Turkey

ABSTRACT

In this study, to combine the biological properties of lanolin and the advantages of electrospun nanofiber mats for developing a potent topical wound dressing/nursing pads that includes lanolin, lanolin incorporated electrospun cellulose acetate (CA), polyethylene oxide (PEO), polyethylene oxide/chitosan (PEO/chitosan) and thermoplastic polyurethane (TPU) nanofibers were developed and characterized. Surface tension, viscosity and conductivity measurements of each polymer solution were carried out in order to characterize the spinning solutions. Lanolin addition did not affect the conductivity values but increase the viscosity of each spinning solution. According to the SEM images, smooth nanofiber surfaces were produced which could be appropriate for a top layer of a nursing pad. Slightly attached, thicker nanofibers could be seen from the TPU/Lanolin images. Similar to TPU nanofibers, CA nanofibers were smoother and thinner than CA/Lanolin nanofibers. Lanolin effected the uniformity of the PEO nanofibers, but it could be said that homogeneous distribution of lanolin was achieved. Characterization of these nanofiber membranes were also carried out with FTIR, DSC, swelling and weight loss analysis. Since TPU nanofibers were hydrophobic and the addition of lanolin made the nanofiber more hydrophobic, they did not show high swelling ratios. CA nanofibers swelled 610% due to their relatively hydrophilic nature and bulky structure. PEO nanofibers were totally dissolved in the water, a very thin layer remained for PEO-Chitosan/lanolin nanofibers. So, using electrospun CA and TPU nanofiber membranes for a nursing pad upper layer could be suitable. CA/lanolin nanofibers showed better hydrophilicity and swelling when compared to TPU nanofibers. On the other hand, TPU nanofibers are more elastic and durable with lower swelling.

ARTICLE HISTORY

Received 12 May 2022
Accepted 10 October 2022

KEYWORDS

Lanolin; nursing pads;
nanofibers; electrospinning

1. Introduction

The use of electrospun nanofibers for the development of innovative topical medical materials is of great interest due to their smooth surface, softness, porosity and high surface-to-volume ratios (Çay et al., 2017; Miguel et al., 2019). Nanofibers has the ability to carry therapeutics such as anti-microbial agents and wound healing enhancers (Aramwit, 2016). Thus, they are considered as potential candidates for biomedical applications such as drug delivery, scaffolding, wound applications. Cell attachment and proliferation are the important factors in wound healing. With high surface area and microporous structure, the nanofiber membranes could quickly start signaling pathway and attract fibroblasts to the derma layer (Chen et al., 2008) that enhance the wound healing. Collagen (Rath et al., 2016; Rho et al., 2006), poly(lactide-co-glycolide), poly(ϵ -caprolactone), poly(ethyleneglycol) (Choi et al., 2008), chitosan (Zarghami et al., 2015; Zhang et al., 2019), polyvinyl alcohol (Zhang et al., 2019), cellulose acetate (Elsayed et al., 2020; Lee & Lee, 2020; Liu et al., 2020), polyurethane (Sofi et al., 2019), composite thermoplastic polyurethane (Kim et al., 2016; Mistry

et al., 2021; Samimi Gharai et al., 2018), chitosan/polyethylene oxide nanofibers (Kalalinia et al., 2021) are commonly studied nanofibers for wound applications. Some active agents such as antibiotics (Kalalinia et al., 2021; Katti et al., 2004), silver nanoparticles (Rath et al., 2016), natural extracts-derived products (Kharat et al., 2021; Lee & Lee, 2020; Liu et al., 2020; Sofi et al., 2019) and the molecules capable of enhancing the healing process such as growth factors (Choi et al., 2008), vitamins (Fathi-Azarbayjani et al., 2010; Taepaiboon et al., 2007), and anti-inflammatory agents (Akduman et al., 2016, 2018; Kenawy et al., 2007; Shi et al., 2013; Taepaiboon et al., 2006) could be loaded to polymeric nanofibers for wound healing purposes.

Lanolin is an animal wax, devoid of glycerides, which is secreted from the sheep and other animals and has long been recognized as an effective moisturizer for the skin. About 2 to 3 mg cm⁻² of lanolin is readily absorbed by the stratum corneum with no residual surface film (Clark, 1992). It mainly consists of mono-, di-, and poly-hydroxyl esters of sterols, trimethyl, triterpene alcohols, aliphatic alcohols (C14–C37), and free hydrocarbons. The

biocompatibility of lanolin has been attributed to its similar chemical nature as that of human sebum (Sagiri et al., 2013). Lanolin creates an air-permeable temporary barrier and promotes moist wound healing when applied to injured skin. It is proven to have anti-inflammatory, antimicrobial, skin-protecting and barrier repair properties (Abou-Dakn et al., 2011; Harris & Hoppe, 2006).

The use of lanolin as a nipple treatment has been normalized by retail marketing and healthcare providers (Sasaki et al., 2014). Nipple pain and/or trauma associated with breastfeeding are common, and are cited as one of the main reasons for early cessation of breastfeeding in the early postpartum period (Abou-Dakn et al., 2011; Harris & Hoppe, 2006; Sasaki et al., 2014; Tait, 2000). A variety of interventions have been used to either treat or prevent nipple pain. These include topical creams, solutions or sprays which may include lanolin as an active substance. Various brands of lanolin nipple cream are sold at retailers and dispensed by healthcare personnel for breastfeeding mothers as a treatment for sore and cracked nipples. A pea-sized amount of lanolin is applied after each feeding to soothe and protect sore, dry, and cracked nipples. However, one of the main disadvantages is that, after each application, most of the lanolin is absorbed by either a nonwoven disposable nursing pad or a vest or a bra. This causes the sticking of the nipples to the material in contact, which resulted more pain.

Nanofiber mats prepared by the electrospinning method have unique properties. This study is the prime motivation behind being a starting point of the development of electrospun nanofibers functionalized by lanolin for potential applications in cracked nipples treatments since lanolin incorporation into nanofibers as an upper layer would alter the properties and utility of the nursing pads. Lanolin incorporated nanofiber mats prepared by the electrospinning method will deliver the lanolin to the cracked nipples, will provide smooth and soft high specific surface area and high porosity with fine pores which will also lead to improved wicking properties. Nanofiber surface would also prevent the sticking of the nipples to the surface of the nursing pad because of the smoother surface. These properties make lanolin incorporated nanofibers as a potential layer for disposable nursing pads. In the contrary to traditional lanolin creams which are needed to be applied several times during the day, it is expected that lanolin incorporated nanofiber mats that could be placed in the center of a nursing pad, will promote the wound healing. The design and production of lanolin incorporated nanofiber-based materials produced by electrospinning is of interest for use in innovative topical applications.

In this paper the results of the development of lanolin incorporated electrospun cellulose acetate (CA), poly(ethylene oxide) (PEO), polyethylene oxide/chitosan (PEO/Chitosan) and thermoplastic polyurethane (TPU) nanofibers were given. CA is a derivative of the naturally occurring raw material and is an alternative to synthetic polymers produced from petroleum (Nicosia et al., 2016). CA nanofibers could be utilized for various applications ranging from affinity membranes (Ma et al., 2005) to tissue engineering (Liu

et al., 2012; Luo et al., 2013) and sensors (Hu et al., 2017). CA was chosen because of its high hydrophilicity, good liquid permeability and water absorption capacity (Nicosia et al., 2016; Zhou et al., 2011). CA is also stable to water and has good solubility in organic solvents (Zhou et al., Omollo et al., 2016). PEO is one of the major classes of synthetic polymer hydrogels. It has been approved by the Food and Drug Administration for several medical applications (Kumar & Erothu, 2017). PEO was chosen because of its biocompatibility, low toxicity and high hydrophilicity. Besides, chitosan has a number of potential commercial and biomedical uses including bandages to reduce bleeding and as an antibacterial agent (Kumar & Erothu, 2017). It can be used to help deliver drugs through the skin in medical applications (Silva et al., 2008). TPU was also chosen because of its good biocompatibility, high mechanical properties and easy electrospinnability (Çay et al., 2015). Its biocompatibility, nontoxicity, toughness and functionality have led to the widespread use of TPU in implantable devices (vascular grafts, pacemaker leads, blood bags, bladders and artificial heart valves) and medical applications (Gupta & Edwards, 2009; Huynh et al., 2010; Zdrachala & Zdrachala, 1999). In addition, it is possible to obtain smooth and fine nanofibers from CA, PEO, PEO/Chitosan and CA *via* electrospinning. To the best of our knowledge, the electrospinning of Lanolin incorporated nanofibers has not yet been investigated before. All these four polymers were selected because of their biocompatibility and after swelling and weight loss studies, it would be possible to evaluate which combination will be more suitable for a nursing pad layer and for cell biocompatibility assessment. This is the first study about lanolin loaded nanofibers and clearly defines the production of four lanolin loaded nanofibers. Thus, the main objective of the present study is to develop and characterize novel electrospun nanofibrous materials containing lanolin. Furthermore, surface tension, viscosity and conductivity measurements of each polymer solutions were carried out in order to characterize the spinning solutions. The surface morphology of electrospun lanolin incorporated CA, TPU and PEO nanofibers were investigated by SEM imaging. Characterization of these nanofiber membranes were carried out with FTIR, DSC, swelling, weight loss analysis.

2. Experimental

2.1. Materials

The TPU (Pellethane 2103-80AE) used in this study is based on 4,4-methylene bisphenylene isocyanate, polytetramethyleneoxide and 1,4 butanediol, and was provided from Velox (Lubrizol Advanced Materials). PEO (Polyox WSR N750) is a trademark of Dow Chemical Company, with approximate molecular weight of 300,000. It was provided Hifyber as a gift. CA with number average molecular weight of ~30,000 g/mol and acetylation degree of 39.8 wt. % and 75–85% deacetylated Chitosan with medium molecular weight were purchased from Sigma Aldrich Chemical Company. Lanolin, acetone, dimethylacetamide (DMAc), N,Ndimethylformamide (DMF), chloroform, tetraethylammonium bromide (TEAB) and

Table 1. Polymer concentration, solvents and Lanolin percentages.

	Polymer Concentration	Lanolin Percentage W/W _{polymer}	Polymer amount (g)	Lanolin (g)	Solvent Type	Solvent amount for each polymer (g)
TPU	~8.5% (w/w)		3 g		DMF	32 g
TPU/Lanolin	~8.5% (w/w)	30%	3 g	0.9	DMF/Chloroform	27 g/5 g
CA	16% (w/w)		6.4 g		Acetone/DMAc	22.4g/11.2g
CA/Lanolin	16% (w/w)	30%	6.4 g	1.92	Acetone/DMAc	22.4g/11.2g
PEO	8% (w/w)		3.2 g		distilled water	36.8 g
PEO/Lanolin	8% (w/w)	30%	3.2 g	0.96	distilled water	36.8 g
PEO-Chitosan	~2.67% w/w PEO- %1 w/w Chitosan		0.4 g PEO- 0.15 g Chitosan		%50 Acetic Acid	4.6 g- 4.85 g- 5g
PEO-Chitosan /Lanolin	~2.67% w/w PEO- 1% w/w Chitosan	30%	0.4 g PEO- 0.15 g Chitosan	0.165	%50 Acetic Acid	4.6 g- 4.85 g- 5g

(Note: Total polymer solution amounts were; 35 g for TPU and TPU/Lanolin, 40 g for CA and CA/Lanolin, 40 g for PEO and PEO/Lanolin and 15 g for PEO-Chitosan and PEO-Chitosan/Lanolin solutions).

Triton X-100 were also purchased from Sigma Aldrich Chemical Company.

2.2. The preparation of neat and lanolin incorporated electrospinning solutions

Neat TPU, CA, PEO and PEO-Chitosan solutions were prepared according to Table 1. Then 30%wt. lanolin, based on polymer weight was added to each electrospinning solution. Detailed preparations were given below.

Neat TPU solution was prepared by dissolving TPU granules in the concentration of %8.5 (w/w) in DMF at room temperature. Solution was stirred with a magnetic stirrer for 12 h. For the preparation of TPU/Lanolin solution, first lanolin was dissolved in chloroform, and this lanolin solution was added to the 10% (w/w) TPU solution and stirred for further 2 h. Final TPU and TPU/Lanolin solutions' TPU concentration was both ~8.5% (w/w). CA solution was prepared by dissolving CA powder in the concentration of 16% w/v in acetone/DMAc in the volume ratio of 2:1 at 50 °C and stirred for 3 h. For the preparation of CA/Lanolin solution, the 16% (w/w) CA solution was directly added on the weighed amount of lanolin and stirred for further 2 h with a magnetic stirrer. PEO solution was prepared by dissolving PEO powder in the concentration of 8% w/w in distilled water and stirred for 2 h at 50 °C than cooled down to the room temperature and stirred further 2 h. For the preparation of PEO/Lanolin solution, first lanolin was dispersed in 50 °C of distilled water and PEO powder was added to this lanolin dispersed solution and stirred for 2 h at 50 °C and cooled down to the room temperature again. To prepare PEO-Chitosan solution, 5 g PEO solution (8% w/w), 5 g chitosan solution (3% w/w) and additional 5 g acetic acid (50% v/v) were mixed to prepare PEO/chitosan solution. 0.275 g non-ionic surfactant Triton X-100 (Bhattacharai et al., 2005) and organic salt TAEB (Akduman et al., 2018; Topuz et al., 2021) were added to the PEO-Chitosan solution for better spinnability. For PEO-Chitosan/Lanolin solution lanolin was dissolved in acetic acid (50% v/v) and added into the PEO-Chitosan solution mixture. Final polymer concentrations, lanolin percentages, polymer and lanolin amounts, solvent type and solvent amount of each polymer were given in Table 1.

2.3. Electrospinning of neat and lanolin incorporated nanofibers

Electrospinning of the polymer solutions was carried out by a set-up consisting a flat tip stainless steel needle, grounded rotating metal drum collector and a high voltage supply. TPU, CA, PEO and PEO-chitosan solutions were electrospun at voltages of 13, 15, 15, 15 kV and tip-to-collector distances of 18, 15, 15, 15 cm, respectively. Feeding rates of 0.4–0.5 ml/h were used for all solutions. 90 mesh plain woven monofilament 100% polyester fabric was used as a deposition material for easy separation of nanofibers

2.4. Characterization

2.4.1. Characterization of electrospinning solutions

Viscosity of the solutions was measured by using Brookfield DV-III Rheometer with a spindle type SC4-21 at 30 rpm. Surface tension measurement was carried out by Krüss Easy Dyne Analyser by Plate Method. Conductivity measurement was carried out using J.P. Selecta Conductivity meter, CD-2004.

2.4.2. SEM analysis

The morphologies of TPU, TPU/Lanolin, CA, CA/Lanolin, PEO and PEO/Lanolin nanofibers before and after wetting and drying were characterized using scanning electron microscopy (SEM, Phenom G2pro). Each sample was sputtered by Quorum Q150R S ion sputtering device with a thin layer of gold prior to SEM observation. The mean diameter of the nanofibers was calculated from the measurements on SEM images of 5000× magnification by using Image J program. Approximately fifty measurements were carried out from different parts of each sample.

2.4.3. FT-IR analysis

Fourier transform infrared spectroscopy (FT-IR) analyses were carried out with Perkin Elmer FT-IR spectrometer for TPU, TPU/Lanolin, CA, CA/Lanolin, PEO and PEO/Lanolin nanofibers and lanolin. Scans were obtained in a spectral range from 650 to 4000 cm⁻¹ with a resolution of 1 cm⁻¹ for neat and lanolin incorporated nanofibers.

2.4.4. Thermal properties of nanofibrous mats

Thermal behaviors of neat and lanolin incorporated nanofibers were investigated by differential scanning calorimetry (DSC) (TA Instrument, Q10 DSC instrument). Neat and lanolin incorporated nanofibers were sealed in alumina pan and heated under a continuous nitrogen purge at the rate of 50 ml/min, samples were scanned at a heating rate of 10 °C/min between 0 and 350 °C (Taepaiboon et al., 2006; TA Instrument, Model DSC Q10).

2.4.5. Swelling and weight loss

The percentage of swelling and weight loss of the TPU, TPU/Lanolin, CA, CA/Lanolin, PEO, PEO/Lanolin, PEO-Chitosan and PEO-Chitosan/Lanolin nanofiber mats were measured upon exposure in distilled water. The samples were removed from the medium after 24 h and carefully blotted with tissue paper to remove excess water from the surface. The weight changes due to the water uptake determined, then the samples were dried at room temperature. Degree of swelling and weight loss were calculated according to the following equations:

$$\text{Degree of swelling (\%)} = \frac{M - M_d}{M_d} \times 100 \quad (1)$$

and

$$\text{Weight loss (\%)} = \frac{M_i - M_d}{M_i} \times 100 \quad (2)$$

where M is the weight of each nanofiber mat after immersion in distilled water (wet weight) for 24 h, M_d is the weight of the sample in dried state (dried weight), M_i is the initial weight of the sample (Akduman et al., 2018; Özgüney et al., 2009).

3. Results and discussion

Processing parameters and polymer solution properties such as applied voltage, polymer feeding rate, tip to needle distance, surface tension, solution viscosity and conductivity have an effect on resultant fiber morphology. Surface tension, solution viscosity and conductivity results of neat and lanolin loaded polymer solutions were compared and given in Table 2. The charges on the polymer solution should overcome the viscosity and surface tension of the polymer solution to form an electrospinning jet. Surface tension is generally considered the change in surface free energy per unit increase in surface area (Ramakrishna et al., 2005). Due to the strong intermolecular hydrogen bonding, water has high surface tension about 72.8 mN/m at room temperature (Huang et al., 2011). When PEO was added to the water, the intermolecular forces became weaker (Kim, 1997) and decreased the surface tension to 53.1 mN/m. Additionally, because of the hydrophobic behavior and high surface activity of lanolin (Harris & Hoppe, 2006), lanolin addition decreased the surface tension of PEO/lanolin solution to 40.6 mN/m. Furthermore, preparing the solution in acetic acid and adding chitosan decreased the surface tension of the solution to 36.3 mN/m. In case of TPU/Lanolin and CA/

Table 2. Surface tension, conductivity and viscosity results of TPU, TPU/Lanolin, CA, CA/Lanolin, PEO and PEO/Lanolin solutions.

Solution	Surface Tension (mN/m)	Conductivity ($\mu\text{S}/\text{cm}$)	Viscosity (cP)
TPU	38.5	2.71	1100
TPU/Lanolin	37.5	2.17	1900
CA	28.8	6.0	700
CA/Lanolin	30.4	6.1	3800
PEO	53.1	132.0	1160
PEO/Lanolin	40.6	129.1	3000
PEO-Chitosan	36.3	1291	4040
PEO-Chitosan /Lanolin	37.9	1254	4400

Lanolin solutions, lanolin was dissolved in chloroform and in acetone/DMAC, respectively. Dissolved lanolin in chloroform and in acetone/DMAC system did not change the intermolecular forces and did not significantly affect the surface tension of the TPU/Lanolin and CA/Lanolin solutions and surface tensions were 37.5 and 30.4 mN/m, respectively.

Another important parameter for electrospinning is the conductivity of the polymer solution. In order to initiate the electrospinning process, applied electrostatic force should be higher than the surface tension of the solution. Thus, a high-power supply is applied to the polymer solution to provide sufficient charges that are able to overcome the surface tension and stretch the solution (Ramakrishna et al., 2005). A minimal electrical conductivity in the solution is therefore essential for electrospinning (Andrady, 2008) and it is determined by the potential for bulk motion of ions in the solution (Stanger et al., 2005). However, one of the other most important electrospinning parameters is related to the extent of chain overlap and entanglement of polymer chains in solution, so electrospinning can occur with moderately concentrated solutions, as the process of jet formation relies on the entanglement (Andrady, 2008). Therefore, even very low conductivities were in case such as TPU, TPU/Lanolin, CA and CA/Lanolin solutions, smooth and fine nanofibers were able to produced. Besides, since lanolin did not have an ionic character, lanolin addition did not change the conductivity values. PEO is a non-ionic polymer and Angamma and Jayaram (2011) measured 7.68 $\mu\text{S}/\text{mm}$ for 5% (w/w) PEO/water solution and with the addition of 2.5 g of salt, conductivity of the PEO solutions increased up to 300 times of initial measurement (2011). But PEO that we used was a commercial product and it might have some impurities, therefore, conductivity values of PEO and PEO/Lanolin solutions were measured 132.0 and 129.1 $\mu\text{S}/\text{cm}$, respectively. On the other hand, PEO-Chitosan solution conductivity was measured 1291 $\mu\text{S}/\text{cm}$. The presence of acetic acid as a solvent and the addition of TAEB significantly increased the conductivity of the solution (Akduman, 2019; Topuz et al., 2021).

Despite the high conductivity and the relatively low surface tension of PEO-Chitosan solution, medium molecular weight of chitosan which causes the high viscosity resulted difficulty in electrospinning. Sufficient molecular weight of the polymer is essential for electrospinning but polymer solution should have appropriate viscosity. During electrospinning process, the polymer solution is stretched between

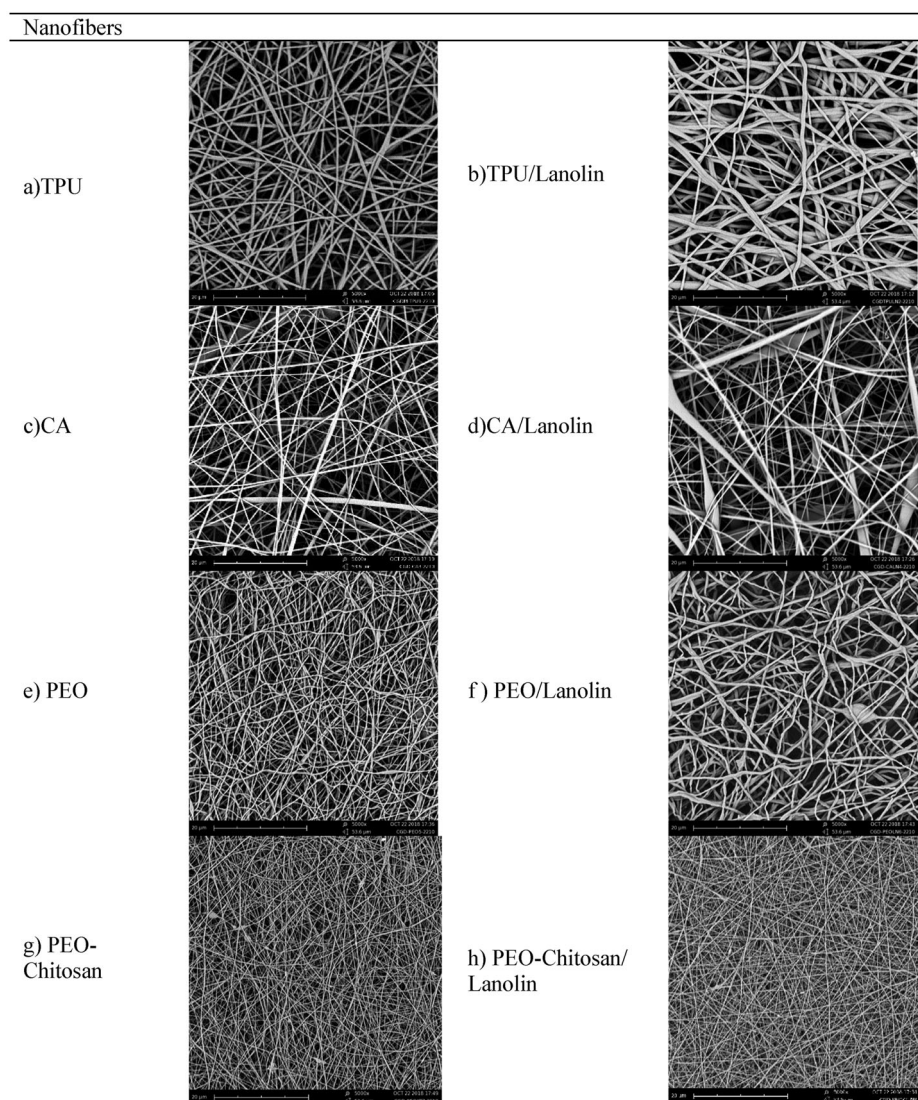


Figure 1. SEM images (5000x) a) TPU, b) TPU/Lanolin, c) CA, d) CA/Lanolin, e) PEO and f) PEO/Lanolin, g) PEO-Chitosan, h) PEO-Chitosan/Lanolin nanofibers.

the tip and the collector (Ramakrishna et al., 2005) and the entanglement of the polymer chains prevents jet break-up and maintains continuous polymer jet that forms nanofibers. The molecular weight of the polymer and the polymer concentration have an effect on the viscosity which determine the amount of entanglement of the polymer chains in the solvent. In this study, the viscosity of the 8.5% TPU, 16% CA, 8% PEO and 2.67/1% PEO-Chitosan solutions were 1100, 700, 1160 and 4040 cP, respectively. Except PEO-Chitosan solution all three-solution viscosity were appropriate for electrospinning and smooth nanofibers were obtained. However, chitosan polymer has a deacetylation degree of 75–85% and it has a medium molecular weight. Therefore, even with 1% w/w chitosan solution, very high viscosity was obtained and that resulted in high viscosity of PEO-Chitosan solution which was difficult to spin. When the viscosity was too high, it was very hard to pump the solution and the polymer solution often dried at the tip of the needle and resulted in very low productivity.

In order to produce lanolin incorporated TPU nanofibers first lanolin was dissolved in chloroform and added to the TPU solution. Because of the waxy structure at room

temperature, the viscosity of the TPU/Lanolin solution increased to 1900 cP. Lanolin was also soluble in acetone and directly added to the CA solution but it again increased the viscosity of the CA solution from 700 cP to 3800 cP. The amount of lanolin in the CA/Lanolin solution was higher because the percentage of lanolin was calculated on the polymer weight and the amount of CA polymer was higher than that of TPU. Therefore, the viscosity increase of the CA/Lanolin solution was higher than the TPU/Lanolin solution. Lanolin has a melting point of $\sim 38^{\circ}\text{C}$ and is insoluble in water and acetic acid, thus PEO and PEO-Chitosan solutions were heated to $40\text{--}45^{\circ}\text{C}$ and lanolin was directly dispersed in these warm solutions. However, when they were cooled down to the room temperature, solutions became more viscous. Lanolin is a kind wax and solid at room temperature, it significantly increased the viscosity of all polymer solution especially TPU, CA and PEO which also resulted in relatively thicker nanofibers. Because of low polymer concentration used for PEO-Chitosan solution, produced nanofibers were thinner than TPU, CA and PEO nanofibers.

According to the visual assessments of SEM images, smooth nanofiber surfaces were produced which could be

Table 3. The mean diameters (nm), mean thickness (mm) and mean weight (g/m^2) results of TPU, TPU/Lanolin, CA, CA/Lanolin, PEO and PEO/Lanolin, PEO-Chitosan, PEO-Chitosan/Lanolin nanofibers.

Nanofibers	Mean Nanofiber Diameters (nm) \pm SD	Mean Thickness (mm) \pm SD	Weight (g/m^2)
TPU	397.73 \pm 86.71	0.19 \pm 0.029	52.83
TPU/Lanolin	599.13 \pm 169.74	0.20 \pm 0.030	67.64
CA	319.56 \pm 140.24	0.28 \pm 0.023	85.67
CA/Lanolin	424.01 \pm 241.15	0.46 \pm 0.055	101.45
PEO	257.93 \pm 64.69	0.04 \pm 0.010	23.38
PEO/Lanolin	493.22 \pm 128.60	0.07 \pm 0.013	42.52
PEO-Chitosan	184.86 \pm 60.76	0.02 \pm 0.008	7.00
PEO-Chitosan/Lanolin	181.88 \pm 34.52	0.01 \pm 0	1.88

appropriate for a top layer of a nursing pad. The SEM images of TPU, TPU/Lanolin, CA, CA/Lanolin, PEO and PEO/Lanolin nanofibers were given in Figure 1. Slightly attached, thicker nanofibers could be seen from the TPU/Lanolin images (Figure 1b). Lanolin addition negatively affected the smoothness of the TPU nanofibers. Similar to TPU nanofibers, CA nanofibers were smoother and thinner than CA/Lanolin nanofibers. From the 1000x images (Supplementary file, Figure S1), more defects could be seen for CA/Lanolin nanofibers. In case of PEO/Lanolin nanofibers, lanolin effected the uniformity of the PEO nanofibers, but it could be said that homogeneous distribution of lanolin was achieved. In Table 3, the mean diameters (nm), the mean thickness (mm) and the mean weight (g/m^2) results of TPU, TPU/Lanolin, CA, CA/Lanolin, PEO and PEO/Lanolin nanofibers were given. Related to the viscosity of the solutions, lanolin addition significantly increased the nanofiber diameters. TPU and TPU/lanolin nanofibers were produced in the range of 397.73 and 599.13 nm, CA and CA/Lanolin nanofibers were produced in the range of 319.56 and 424.01 nm and PEO and PEO/Lanolin nanofibers were produced in the range of 257.93 and 493.22 nm. In TPU nanofibers, lanolin did not significantly affect the thickness of the mats however, for CA/Lanolin and PEO/Lanolin nanofibers, produced nanofiber mats were thicker than that of CA and PEO nanofiber mats. The PEO-Chitosan solution consisted of 2.67% PEO and 1% chitosan and produced nanofiber diameters were about 184 nm. Since 30% lanolin was added to each polymer solution on polymer weight, PEO-Chitosan/Lanolin solution consisted relatively low lanolin amount which did not affect the nanofiber diameter significantly. Due to the high productivity of the TPU and CA nanofibers, produced mats had relatively high weight than PEO and PEO-Chitosan nanofibers. Especially, because of the spinning difficulty and low productivity of the PEO/Chitosan solution, produced mat was about 7.0 g/m^2 and PEO-Chitosan/Lanolin was about 1.88 g/m^2 .

3.1. FTIR results

FTIR spectrums of neat and lanolin loaded TPU, CA, PEO and PEO-Chitosan nanofibers were given in Figures 2–5, respectively. Lanolin contains fatty esters (14–24%), sterols and triterpene alcohol esters (45–65%), free alcohols (6–20%), sterols (cholesterol, lanosterol) and terpenes

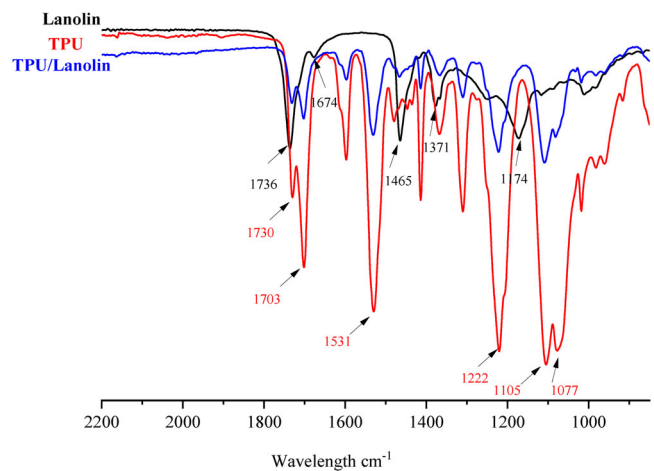


Figure 2. FTIR spectrum of lanolin, TPU nanofibers, TPU/Lanolin nanofibers.

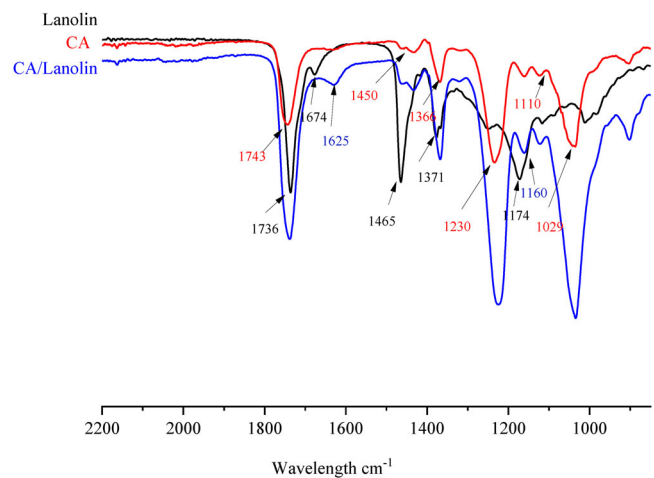


Figure 3. FTIR spectrum of lanolin, CA nanofibers ve CA/Lanolin nanofibers.

(4–5%) (Yilmaz et al., 2020). Hydroxylated fatty acids (mainly hydroxy palmitate) are found either free or esterified. Fatty acid chains have from 14 up to 35 carbon atoms, many of them having branched chains (iso or anteiso conformations). FTIR spectrum of lanolin showed a peak at about 1736 cm^{-1} due to the stretch of carbonyl bond ($\text{C}=\text{O}$) of ester groups, a vibrating group of aromatic $-\text{COOH}$ at 1674 cm^{-1} that could be assigned to $\nu(\text{C}=\text{O})$, a peak at 1465 cm^{-1} of methylene $\delta(\text{CH}_2)$, a peak at 1371 cm^{-1} of methyl $\delta_s(\text{CH}_3)$ vibrations of aliphatic hydrocarbons and a peak at 1174 cm^{-1} of $\text{C}-\text{O}-\text{C}$ bonds (Niculescu et al., 2015; Masae et al., 2014; Figure 2).

The TPU used in this study was the commercial Pellethane 2103-80AE, which is based on 4,4-methylene bisphenylene isocyanate, polytetramethyleneoxide and 1,4 butanediol. In Figure 2, key TPU peaks were observed at approximately 1730 and 1703 cm^{-1} indicating the carbonyl stretching of the urethane groups (McCarthy et al., 1997; Tanzi et al., 1997; Wilhelm et al., 1998). At 1531 cm^{-1} the N-H bending and C-N stretching (Huynh et al., 2010), at 1414 cm^{-1} the C-C benzene stretching, at approximately 1222 cm^{-1} the C-N stretching and at approximately 1105 cm^{-1} the ether absorbance was also observed (McCarthy et al., 1997). The FTIR spectrum of TPU/Lanolin

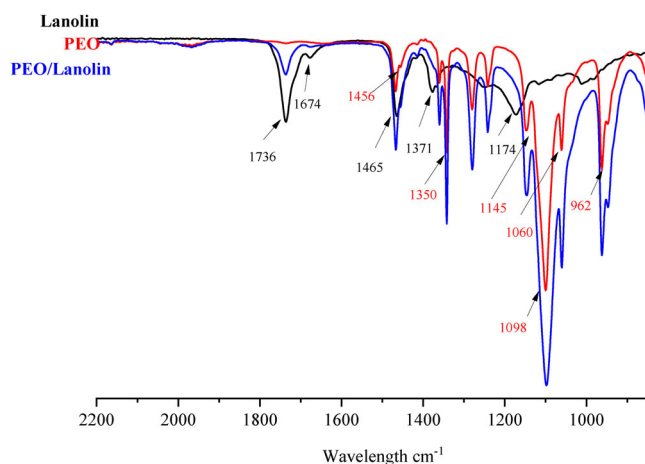


Figure 4. FTIR spectrum of Lanolin, PEO and PEO/Lanolin nanofibers.

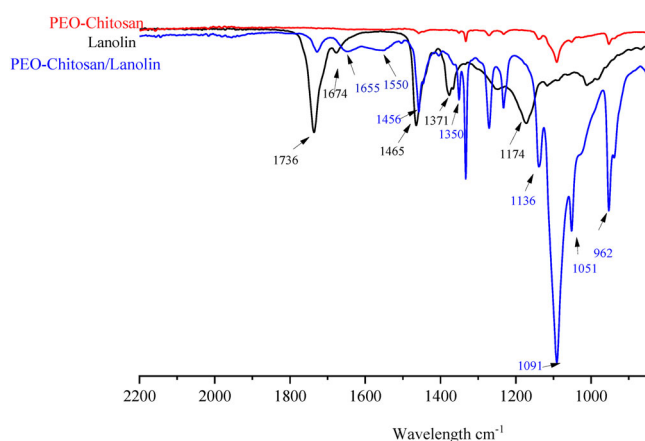


Figure 5. FTIR spectrum of lanolin, PEO-Chitosan and PEO-chitosan/lanolin nanofibers.

nanofibers was similar to the spectrum of TPU nanofibers. Characteristic peaks of TPU at 1730, 1703, 1531, 1222 and 1105 cm^{-1} could be seen.

FTIR spectrums of lanolin, CA and CA/Lanolin nanofibers were given in Figure 3. Characteristics peaks of CA nanofibers at 1743 cm^{-1} was attributed to the carbonyl stretching ($\text{C}=\text{O}$) (Ma et al., 2005; He, 2017), vibrations at 1450 cm^{-1} were attributed to $\text{O}=\text{C}-\text{OR}$ (Ding et al., 2004), the vibrational modes at 1366 cm^{-1} were attributed to C-H deformations of the carbon chain of cellulose acetate [64], peak at 1230 cm^{-1} to acetyl ester group ($\nu\text{CH}_3-\text{C}=\text{O}$) (He, 2017), and 1110 cm^{-1} and 1029 cm^{-1} could be attributed ether groups ($\text{C}-\text{O}-\text{C}$) (De Moraes et al., 2015; Ding et al., 2004). FTIR spectrum of CA/Lanolin nanofibers was also similar to the CA nanofibers but stretch of aromatic carbonyl bond $-\text{COOH}$ carbonyl $\nu(\text{C}=\text{O})$ moved to the 1625 cm^{-1} at CA/Lanolin spectrum. Peak at 1160 cm^{-1} of CA/Lanolin spectrum could be attributed to the ether groups ($\text{C}-\text{O}-\text{C}$).

The FTIR spectra of PEO nanofibers (Figure 4) showed peaks at about 1456 and 1350 cm^{-1} and they were attributed to the vibrations of $-\text{CH}_2-$ group and the bands at about 1098 and 962 cm^{-1} could be assigned to the asymmetric stretching vibration of the C-O group (Ajao et al., 2010). The presence of the crystalline PEO phase was confirmed by

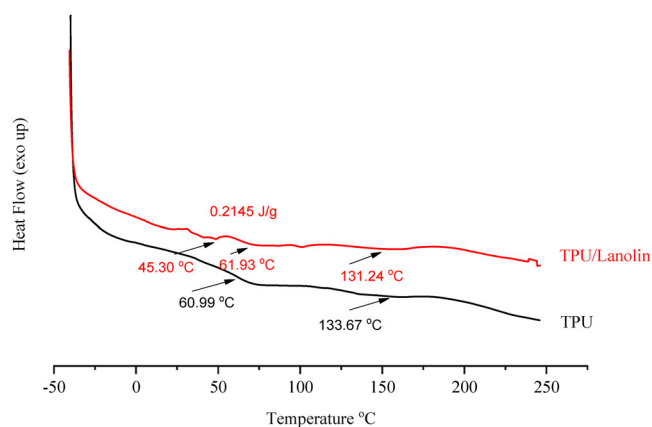


Figure 6. DSC curves of TPU and TPU/Lanolin nanofibers.

the triplet peak of the C-O-C stretching vibration at 1145, 1098, and 1060 cm^{-1} . Changes in the intensity, shape, and position of the C-O-C stretching absorptions indicated conformational structures change (Kriegel et al., 2008; Yong et al., 2014). Characteristic peaks of Lanolin that were carbonyl ($\text{C}=\text{O}$) stretching of ester groups at 1736 cm^{-1} , vibration of aromatic $-\text{COOH}$ at 1674 cm^{-1} , could be also seen on PEO/Lanolin nanofibers' spectrum.

For chitosan, bands at 1655 and 1550 cm^{-1} attributed to the carbonyl $\text{C}=\text{O}-\text{NHR}$ or amide I band and the amine $-\text{NH}_2$ or amide II absorption band were expected, respectively (Kriegel et al., 2008). However, the amount of chitosan was very low in PEO-Chitosan nanofibers, thus these expected peaks could hardly be seen at PEO-Chitosan/Lanolin spectrum. Peaks belong to PEO nanofibers at 1456 and 1350 cm^{-1} could be attributed to vibrations of $-\text{CH}_2-$ group, at 962 cm^{-1} to asymmetric stretching vibration of the C-O group and triplet peak of the C-O-C stretching vibration of 1145, 1098, and 1060 cm^{-1} could be seen at 1136, 1091 and 1051 on PEO-Chitosan/lanolin spectrum (Figure 5). Characteristic peaks of Lanolin that were carbonyl ($\text{C}=\text{O}$) stretching of ester groups at 1736 cm^{-1} , vibration of aromatic $-\text{COOH}$ at 1674 cm^{-1} , were also present on spectrum of PEO-Chitosan/Lanolin nanofibers.

3.2. DSC results

The purpose of DSC analysis is to find the melting behavior of membranes under heat. Because these membranes can be attached to the nursing pad by some kind of heat transfer method and may also need to be sterilized, so the temperature of these processes can be decided according to the DSC analysis. DSC curves of TPU and TPU/Lanolin nanofibers were given in Figure 6. DSC curve of TPU nanofibers showed two glass transition (T_g) at 60.99 and 133.67 $^{\circ}\text{C}$ and these endothermic peaks were related to the soft and the hard segments, respectively (Barick & Tripathy, 2010). DSC curve of TPU/Lanolin nanofibers, in the given temperature range, showed a melting at $\sim 45.30^{\circ}\text{C}$ depending on the melting point of Lanolin and enthalpy belonged to this melting is about 0.2145 J/kg. Similar to curve of TPU nanofibers, at 61.93 and 131.24 $^{\circ}\text{C}$, two T_g could be seen. The

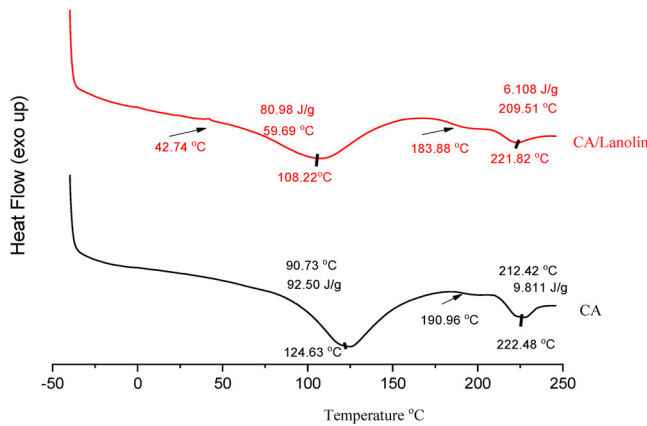


Figure 7. DSC curves of CA and CA/Lanolin nanofibers.

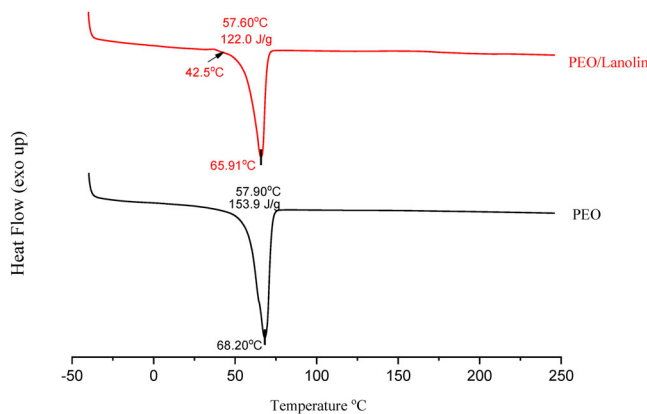


Figure 8. DSC curves of PEO and PEO/Lanolin nanofibers.

presence of lanolin, did not have a significant effect on the Tg of TPU nanofibers.

The neat CA nanofibers exhibited two endothermic thermal transitions, a low-temperature endotherm at 90.73 °C (starting with 75, ending with 183 °C, and the energy requirement was 92.5 J/g, peak temperature was 124.63 °C) corresponding to the moisture loss (Beikzadeh et al., 2020; Lee & Lee, 2020) coupled with the glass transition at 190.96 °C, and a high-temperature endotherm corresponding to the melting range of the material was seen at 212.42 °C with a peak temperature of 222.48 °C. It was reported that the glass transition temperature of CA can be found in a wide temperature range (De Moraes et al., 2015) depending on the degree of acetylation of the polymer, and the melting point of CA can vary depending on the polymerization degree of the polymer (Tungprapa et al., 2007). These two endothermic transitions were also seen in the DSC curves of CA and CA/lanolin nanofibers that were given in Figure 7. In case of CA/Lanolin nanofibers, another glass transition was observed at 42.74 °C depending on the melting point of lanolin (Figure 7). The aforementioned low-temperature-endothermy which was observed around 90.73 °C due to moisture loss of CA nanofibers (Tungprapa et al., 2007), was decreased to 59.69 °C with a peak temperature of 108.22 °C in the presence of lanolin and the required energy was decreased from 92.50 J/g to 80.98 J/g. The glass transition temperature (Tg) was 190.96 °C for CA nanofibers and

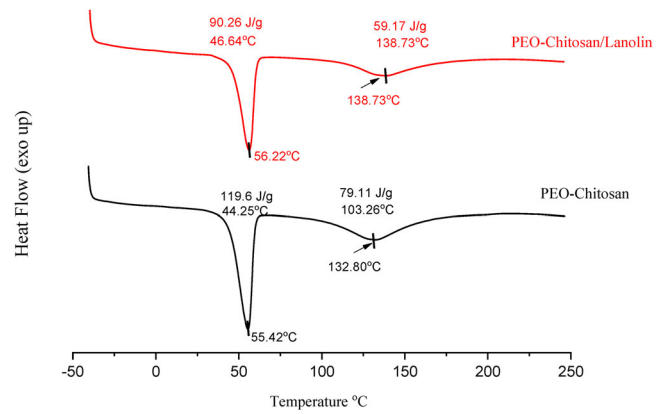


Figure 9. DSC curves of PEO-Chitosan and PEO-Chitosan/Lanolin nanofibers.

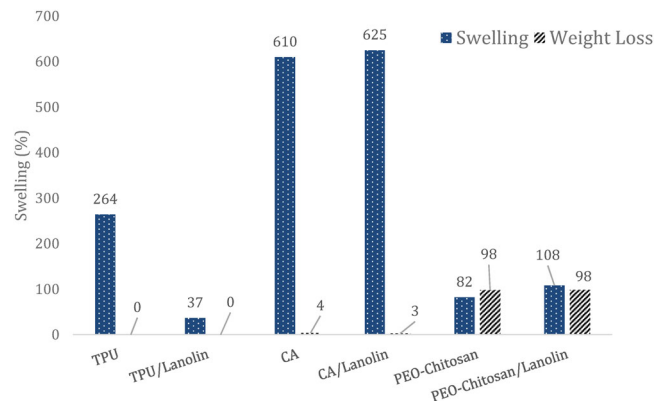


Figure 10. Swelling and weight loss percentages of TPU, TPU/Lanolin, CA and CA/Lanolin and PEO-Chitosan, PEO-Chitosan/Lanolin nanofibers.

183.88 °C for CA/Lanolin fibers. The relatively high Tg indicated the amount and the strength of intra- and intermolecular interactions in the CA chain, while a decrease in Tg means the mobility increase of the polymer (De Moraes et al., 2015). In the presence of lanolin, the melting point was not much changed, decreased from 212.42 °C to 209.51 °C with a peak temperature of 221.82 °C, the amount of energy required for the process decreased from 9.811 to 6.108 J/g.

It was reported that, the melting point of the PEO polymer was observed around 60.7–71.5 °C depending on the molecular weight (Xu et al., 2012; Yong et al., 2014). Besides, both melting point and enthalpy decreased due to the decrease in the crystallinity of the nanofibers after electrospinning. In the DSC curves of the PEO nanofibers (Figure 8), the melting point at 57.9 with a melting peak at 68.2 °C could be seen which were consistent with literature. Energy required for melting was 153.9 J/g. In the presence of lanolin melting point was 57.6 °C with a melting peak at 65.91 °C, not much changed and the enthalpy decreased from 153.9 J/g to 122.0 J/g. Since melting of the PEO started from 36 °C, the melting endotherm of lanolin could hardly be seen and was at 42.5 °C.

DSC curves of PEO-Chitosan and PEO-Chitosan/Lanolin nanofibers were given in Figure 9. Most of the polysaccharides, including chitosan, do not melt due to hydrogen bonds, on the contrary, they decompose above a certain temperature.

Therefore, instead of showing sharp transitions, DSC thermograms show broad endotherms below the decomposition temperature associated with the evaporation of their moisture (Kriegel et al., 2008). The melting point of the carrier polymer PEO, which was used to electrospin chitosan, was observed to be lower than neat PEO nanofibers due to the interactions between PEO and chitosan chains, which prevented the crystallization of PEO (Kriegel et al., 2008). In the DSC curves of the PEO-Chitosan nanofiber, the melting (T_m) was observed at 44.25 °C, with a melting peak at 55.42 °C. In the DSC curves of the PEO nanofibers were given in Figure 8, the T_m

was observed as 57.90 °C. The second endotherm, melting was observed at 103.26 °C with a melting peak at 132.80 °C, and an enthalpy of 79.11 J/g. In case of DSC curves of PEO-Chitosan/Lanolin nanofibers, it was observed that the T_m value of PEO did not change much, but its enthalpy decreased (from 119.6 J/g to 90.26 J/g) due to crystallinity decrease (Kriegel et al., 2008). It was seen that the second endotherm was seen at 112.76 °C and its enthalpy decreased from 103.26 J/g to 59.17 J/g.

The swelling and weight loss results of TPU, TPU/Lanolin, CA, CA/Lanolin and PEO-Chitosan, PEO-Chitosan/Lanolin nanofibers were given in Figure 10. Each nanofiber sample left in distilled water for 24 h. Then, they were carefully blotted with tissue paper to remove excess water from the surface. Since TPU nanofibers were not hydrophilic, they did not show a high swelling ratio (264%). Swelling values were even lower in the presence of lanolin (37%). CA nanofibers swelled 610% due to their relatively hydrophilic nature and bulky structure. No significant change was observed in the presence of lanolin and it was 625%. PEO nanofibers were totally dissolved in the water, so they were excluded from swelling and weight loss analysis. Besides, in case of PEO-Chitosan fibers, a very thin layer remained after 24 h, PEO part was completely dissolved in the aqueous medium. Swelling ratios were 82 and 108% for PEO-Chitosan and PEO-Chitosan/lanolin

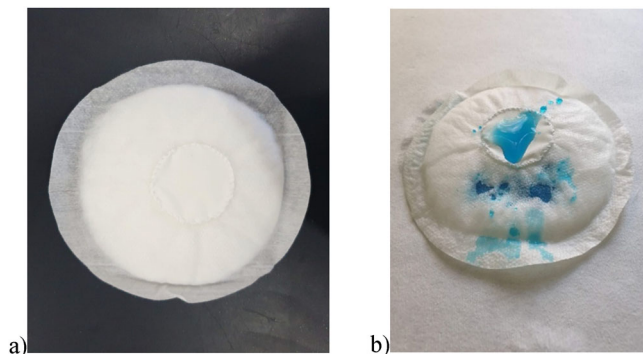


Figure 11. Prototype of a nursing pad with TPU/Lanolin nanofiber in the center, a) before, b) after wetting.

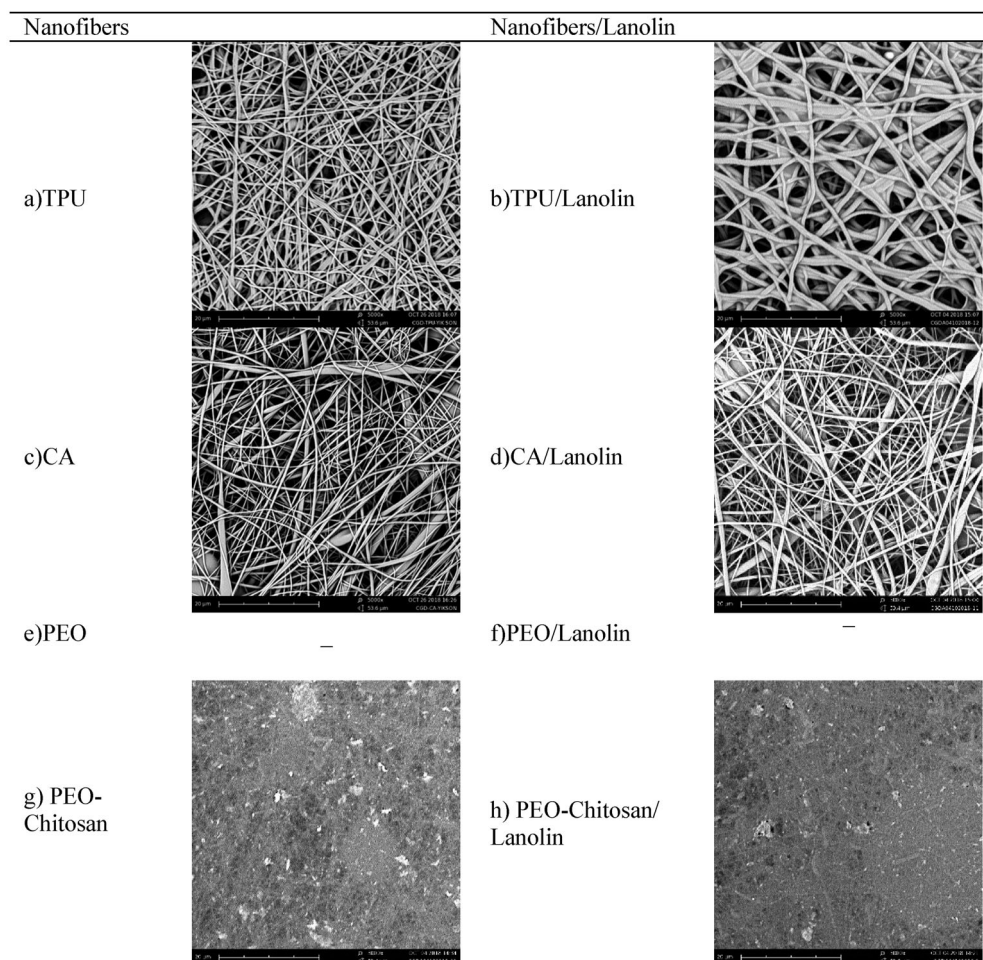


Figure 12. SEM images of (5000x) a) TPU, b) TPU/Lanolin, c) CA, d) CA/Lanolin, e) PEO, f) PEO/Lanolin (g) PEO-Chitosan, h) PEO-Chitosan/Lanolin nanofibers after being kept in distilled water for 24 h.

nanofibers, respectively. Lanolin presence increased the swelling ratio of PEO-chitosan/lanolin nanofibers.

When the weight loss ratios were compared, TPU nanofibers did not show a weight loss as expected, the weight loss observed in CA nanofibers was very low, but, PEO-Chitosan and PEO-Chitosan/Lanolin nanofibers lost 98% of their weight. Therefore, it was concluded that nursing pad design containing PEO nanofibers would not be suitable, using electrospun CA and TPU nanofiber membranes for a nursing pad upper layer could be suitable. CA/lanolin nanofibers showed better hydrophilicity and swelling when compared to TPU nanofibers. On the other hand, TPU nanofibers are more elastic and durable with lower swelling. An example of a nursing pad centered with TPU/lanolin nanofibers presented in Figure 11 could be suggested as a prototype. In this prototype, TPU/lanolin nanofibers can be used as a nursing pad upper surface by using a more hydrophilic layer surrounding the core TPU nanofiber to overcome its low hydrophilicity.

TPU, TPU/Lanolin, CA, CA/Lanolin, PEO, PEO/Lanolin, PEO-Chitosan and PEO-Chitosan/Lanolin nanofibers dried after being kept in distilled water for 24 h. SEM images of these nanofibers were given in Figure 12. TPU nanofibers approached each other and formed lines due to wetting and drying (Supplementary file, Figure S2), other parts did not show significant change except for slight curling. In case of lanolin loaded TPU nanofibers lanolin migrated to the surface and accumulated there due to wetting and drying (Supplementary file, Figure S2). When CA/Lanolin nanofibers were examined, it was observed that lanolin migrated to the surface, similar to TPU/Lanolin nanofibers and they preserved their nanofiber structure. However, the migration of lanolin to the surface was not evaluated as a negative situation, and it was thought that the presence of lanolin on the surface during the use of the nursing pad may be more desirable and may positively affect nipple trauma. On the other hand, since PEO nanofibers were not water resistant, PEO and PEO/Lanolin nanofibers dissolved as soon as they were placed in distilled water, therefore SEM images of these fibers were not available. Only the chitosan parts could be seen from the SEM images of the PEO-Chitosan nanofibers, which remained very thin layer. In the SEM images of PEO-Chitosan/Lanolin nanofibers, Lanolin residues and chitosan fibers could be seen. Due to the low fiber diameter of chitosan nanofibers and the low electrospinning efficiency, produced nanofiber surfaces were also very thin, thus SEM images were not clear enough.

4. Conclusion

In this study, the general information about lanolin, nursing pads and novel electrospun nanofiber mats for nursing pads were summarized. As a potential component for nursing pads, lanolin incorporated electrospun TPU, CA, PEO, and PEO/chitosan nanofibers were developed and characterized. Surface tension, conductivity and viscosity measurements were carried out for each electrospinning solution. According to the SEM images, smooth nanofiber surfaces

were produced which could be appropriate for a top layer of a nursing pad. For same production period, due to the high electrospinning productivity, polymer concentration and the molecular weight of the TPU and CA, TPU and CA nanofibers have the highest thickness and weight. Swelling and weight loss studies showed that, PEO/Lanolin nanofibers would not be suitable as a nursing pad layer because produced mat totally dissolved. In case of PEO-Chitosan/Lanolin nanofibers, produced mat was too thin and since PEO part was dissolved, they did not meet the expected absorbency level. TPU and TPU/Lanolin nanofibers mats showed swelling percentages of ~264% and ~37%, respectively and showed no weight loss. CA and CA/Lanolin nanofibers showed considerable high swelling percentages of ~610% and ~625%, respectively because of more hydrophilic structure and showed very little weight loss. Thus, electrospun CA nanofiber membranes could be preferred when better hydrophilicity and swelling are required. Whenever more elastic and durable mats are required TPU nanofiber mats could also be used with tolerable swelling. For the future studies *in vitro* biocompatibility assessment of lanolin incorporated CA and TPU nanofibers using L929 fibroblasts and HS2 human epithelial cells, the porosity measurements, air and water vapor permeability assessment of Lanolin incorporated TPU nanofibers were planned along with the effect of lanolin amount and deposition time.

Disclosure statement

No potential conflict of interest was reported by the authors.

Funding

This work was supported by the Scientific and Technological Research Council of Turkey (TUBITAK), under Grant [Project No 217M133]. Authors declare patent #2018/16020 pending to Pamukkale and Ege University.

ORCID

C. Akduman  <http://orcid.org/0000-0002-6379-6697>

E. P. Akcakoca Kumbasar  <http://orcid.org/0000-0001-5295-9131>

I. Ozguney  <http://orcid.org/0000-0003-2394-4330>

References

- Abou-Dakn, M., Fluhr, J. W., Gensch, M., & Wöckel, A. (2011). Positive effect of HPA lanolin versus expressed breastmilk on painful and damaged nipples during lactation. *Skin Pharmacology and Physiology*, 24(1), 27–35. <https://doi.org/10.1159/000318228>
- Ajao, J. A., Abiona, A. A., Chigome, S., Fasasi, A. Y., Osinkolu, G. A., & Maaza, M. (2010). Electric-magnetic field-induced aligned electrospun poly (ethylene oxide)(PEO) nanofibers. *Journal of Materials Science*, 45(9), 2324–2329. <https://doi.org/10.1007/s10853-009-4196-y>
- Akduman, C. (2019). PVDF electrospun nanofiber membranes for microfiltration: The effect of pore size and thickness on membrane performance. *European Journal of Science and Technology*, (16), 247–255.
- Akduman, C., Akcakoca Kumbasar, E. P., & Özgüney, I. (2018). Development and characterization of naproxen-loaded poly (vinyl alcohol) nanofibers crosslinked with polycarboxylic acids. *AATCC Journal of Research*, 5(1), 29–38. <https://doi.org/10.14504/ajr.5.1.4>

- Akduman, C., Özgüney, I., & Kumbasar, E. P. A. (2016). Preparation and characterization of naproxen-loaded electrospun thermoplastic polyurethane nanofibers as a drug delivery system. *Materials Science & Engineering: C, Materials for Biological Applications*, 64, 383–390.
- Andrady, A. L. (2008). *Science and technology of polymer nanofibers* (pp. 55–76). John Wiley & Sons.
- Angamma, C. J., & Jayaram, S. H. (2011). Analysis of the effects of solution conductivity on electrospinning process and fiber morphology. *IEEE Transactions on Industry Applications*, 47(3), 1109–1117. <https://doi.org/10.1109/TIA.2011.2127431>
- Aramwit, P. (2016). Introduction to biomaterials for wound healing. In M. S. Ågren (Ed.), *Wound healing biomaterials* (pp. 3–38). Woodhead Publishing.
- Barick, A. K., & Tripathy, D. K. (2010). Thermal and dynamic mechanical characterization of thermoplastic polyurethane/organoclay nanocomposites prepared by melt compounding. *Materials Science and Engineering: A*, 527(3), 812–823. <https://doi.org/10.1016/j.msea.2009.10.063>
- Beikzadeh, S., Akbarinejad, A., Swift, S., Perera, J., Kilmartin, P. A., & Travas-Sejdic, J. (2020). Cellulose acetate electrospun nanofibers encapsulating Lemon Myrtle essential oil as active agent with potent and sustainable antimicrobial activity. *Reactive and Functional Polymers*, 157, 104769. <https://doi.org/10.1016/j.reactfunctpolym.2020.104769>
- Bhattarai, N., Edmondson, D., Veiseh, O., Matsen, F. A., & Zhang, M. (2005). Electrospun chitosan-based nanofibers and their cellular compatibility. *Biomaterials*, 26(31), 6176–6184.
- Çay, A., Kumbasar, E. P. A., & Akduman, Ç. (2015). Effects of solvent mixtures on the morphology of electrospun thermoplastic polyurethane nanofibers. *Tekst Konfeksiyon*, 25(1), 38–46.
- Çay, A., Kumbasar, E. P. A., Keskin, Z., Akduman, Ç., & Ürkmez, A. Ş. (2017). Crosslinking of poly (vinyl alcohol) nanofibers with polycarboxylic acids: Biocompatibility with human skin keratinocyte cells. *Journal of Materials Science*, 52(20), 12098–12108. <https://doi.org/10.1007/s10853-017-1370-5>
- Chen, J. P., Chang, G. Y., & Chen, J. K. (2008). Electrospun collagen/chitosan nanofibrous membrane as wound dressing. *Colloids and Surfaces A: Physicochemical and Engineering Aspects*, 313, 183–188.
- Choi, J. S., Leong, K. W., & Yoo, H. S. (2008). In vivo wound healing of diabetic ulcers using electrospun nanofibers immobilized with human epidermal growth factor (EGF). *Biomaterials*, 29(5), 587–596.
- Clark, E. W. (1992). Short-term penetration of lanolin into human stratum corneum. *Journal of the Society of Cosmetic Chemists*, 43(4), 219–227.
- De Moraes, A. C. M., Andrade, P. F., de Faria, A. F., Simões, M. B., Salomão, F. C. C. S., Barros, E. B., Gonçalves, M. C., & Alves, O. L. (2015). Fabrication of transparent and ultraviolet shielding composite films based on graphene oxide and cellulose acetate. *Carbohydrate Polymers*, 123, 217–227. <https://doi.org/10.1016/j.carbpol.2015.01.034>
- Ding, B., Kimura, E., Sato, T., Fujita, S., & Shiratori, S. (2004). Fabrication of blend biodegradable nanofibrous nonwoven mats via multi-jet electrospinning. *Polymer*, 45(6), 1895–1902. <https://doi.org/10.1016/j.polymer.2004.01.026>
- Elsayed, M. T., Hassan, A. A., Abdelaal, S. A., Taher, M. M., Khalaf Ahmed, M., & Shoueir, K. R. (2020). Morphological, antibacterial, and cell attachment of cellulose acetate nanofibers containing modified hydroxyapatite for wound healing utilizations. *Journal of Materials Research and Technology*, 9(6), 13927–13936. <https://doi.org/10.1016/j.jmrt.2020.09.094>
- Fathi-Azarbayjani, A., Qun, L., Chan, Y. W., & Chan, S. Y. (2010). Novel vitamin and gold-loaded nanofiber facial mask for topical delivery. *AAPS PharmSciTech*, 11(3), 1164–1170.
- Gupta, B. S., & Edwards, J. V. (2009). Textile materials and structures for wound care products. In S. Rajendran (Ed.), *Advanced textiles for wound care* (pp. 48–97). Woodhead Publishing Limited.
- Harris, I., & Hoppe, U. (2006). Chapter 25. Lanolins. In M. Loden & H. I. Maibach (Eds.), *Dry skin and moisturizers* (pp. 309–319). Taylor and Francis.
- He, X. (2017). Fabrication of defect-free cellulose acetate hollow fibers by optimization of spinning parameters. *Membranes*, 7(2), 27. <https://doi.org/10.3390/membranes7020027>
- Hu, L., Yan, X. W., Li, Q., Zhang, X. J., & Shan, D. (2017). Br-PADAP embedded in cellulose acetate electrospun nanofibers: Colorimetric sensor strips for visual uranyl recognition. *Journal of Hazardous Materials*, 329, 205–210. <https://doi.org/10.1016/j.jhazmat.2017.01.038>
- Huang, R., Qi, W., Su, R., Zhao, J., & He, Z. (2011). Solvent and surface controlled self-assembly of diphenylalanine peptide: From microtubes to nanofibers. *Soft Matter*, 7(14), 6418–6421. <https://doi.org/10.1039/c1sm05752a>
- Huynh, T. T. N., Padois, K., Sonvico, F., Rossi, A., Zani, F., Pirot, F., Doury, J., & Falson, F. (2010). Characterization of a polyurethane-based controlled release system for local delivery of chlorhexidine diacetate. *European Journal of Pharmaceutics and Biopharmaceutics: Official Journal of Arbeitsgemeinschaft Fur Pharmazeutische Verfahrenstechnik e.V.*, 74(2), 255–264.
- Kalalinia, F., Taherzadeh, Z., Jirofti, N., Amiri, N., Foroghina, N., Beheshti, M., Bazzaz, B. S. F., Hashemi, M., Shahroodi, A., Pishavar, E., Tabassi, S. A. S., & Movaffagh, J. (2021). Evaluation of wound healing efficiency of vancomycin-loaded electrospun chitosan/polyethylene oxide nanofibers in full thickness wound model of rat. *International Journal of Biological Macromolecules*, 177, 100–110. <https://doi.org/10.1016/j.ijbiomac.2021.01.209>
- Katti, D. S., Robinson, K. W., Ko, F. K., & Laurencin, C. T. (2004). Bioresorbable nanofiber-based systems for wound healing and drug delivery: Optimization of fabrication parameters. *Journal of Biomedical Materials Research Part B: Applied Biomaterials: An Official Journal of The Society for Biomaterials, The Japanese Society for Biomaterials, and The Australian Society for Biomaterials and the Korean Society for Biomaterials*, 70(2), 286–296.
- Kenawy, E. R., Abdel-Hay, F. I., El-Newehy, M. H., & Wnek, G. E. (2007). Controlled release of ketoprofen from electrospun poly (vinyl alcohol) nanofibers. *Materials Science and Engineering: A*, 459(1–2), 390–396. <https://doi.org/10.1016/j.msea.2007.01.039>
- Kharat, Z., Goushki, M. A., Sarvian, N., Asad, S., Dehghan, M. M., & Kabiri, M. (2021). Chitosan/PEO nanofibers containing Calendula officinalis extract: Preparation, characterization, in vitro and in vivo evaluation for wound healing applications. *International Journal of Pharmaceutics*, 609, 121132. <https://doi.org/10.1016/j.ijpharm.2021.121132>
- Kim, M. W. (1997). Surface activity and property of polyethyleneoxide (PEO) in water. *Colloids and Surfaces A: Physicochemical and Engineering Aspects*, 128(1–3), 145–154. [https://doi.org/10.1016/S0927-7757\(96\)03918-0](https://doi.org/10.1016/S0927-7757(96)03918-0)
- Kim, S., Park, S. G., Kang, S. W., & Lee, K. J. (2016). Nanofiber-based hydrocolloid from colloid electrospinning toward next generation wound dressing. *Macromolecular Materials and Engineering*, 301(7), 818–826. <https://doi.org/10.1002/mame.201600002>
- Kriegel, C., Arecchi, A., Arrecchi, A., Kit, K., McClements, D. J., & Weiss, J. (2008). Fabrication, functionalization, and application of electrospun biopolymer nanofibers. *Critical Reviews in Food Science and Nutrition*, 48(8), 775–797.
- Kumar, A. C., & Erothu, H. (2017). Synthetic polymer hydrogels. In R. Francis & D. Sakthi Kumar (Eds.), *Biomedical applications of polymeric materials and composites* (pp. 148–149). Wiley-VCH Verlag GmbH & Co.
- Lee, K., & Lee, S. (2020). Electrospun nanofibrous membranes with essential oils for wound dressing applications. *Fibers and Polymers*, 21(5), 999–1012. <https://doi.org/10.1007/s12221-020-9300-6>
- Liu, X., Lin, T., Gao, Y., Xu, Z., Huang, C., Yao, G., Jiang, L., & Wang, X. (2012). Antimicrobial electrospun nanofibers of cellulose acetate and polyester urethane composite for wound dressing. *J Biomed Mater Res B*, 100(6), 1556–1565.
- Liu, F., Li, X., Wang, L., Yan, X., Ma, D., Liu, Z., & Liu, X. (2020). Sesamol incorporated cellulose acetate-zein composite nanofiber membrane: An efficient strategy to accelerate diabetic wound healing. *International Journal of Biological Macromolecules*, 149, 627–638.

- Luo, Y., Wang, S., Shen, M., Qi, R., Fang, Y., Guo, R., Cai, H., Cao, X., Tomas, H., Zhu, M., & Shi, X. (2013). Carbon nanotube-incorporated multilayered cellulose acetate nanofibers for tissue engineering applications. *Carbohydrate Polymers*, 91(1), 419–427. <https://doi.org/10.1016/j.carbpol.2012.08.069>
- Ma, Z., Kotaki, M., & Ramakrishna, S. (2005). Electrospun cellulose nanofiber as affinity membrane. *Journal of Membrane Science*, 265(1–2), 115–123. <https://doi.org/10.1016/j.memsci.2005.04.044>
- Masae, M., Pitsuwan, P., Sikong, L., Kooptarnond, K., Kongsong, P., & Phoempoon, P. (2014). Thermo-physical characterization of paraffin and beeswax on cotton fabric. *Science & Technology Asia*, 19(4), 69–77.
- McCarthy, S. J., Meijs, G. F., Mitchell, N., Gunatillake, P. A., Heath, G., Brandwood, A., & Schindhelm, K. (1997). In-vivo degradation of polyurethanes: Transmission-FTIR microscopic characterization of polyurethanes sectioned by cryomicrotomy. *Biomaterials*, 18(21), 1387–1409. [https://doi.org/10.1016/S0142-9612\(97\)00083-5](https://doi.org/10.1016/S0142-9612(97)00083-5)
- Miguel, S. P., Sequeira, R. S., Moreira, A. F., Cabral, C. S., Mendonça, A. G., Ferreira, P., & Correia, I. J. (2019). An overview of electrospun membranes loaded with bioactive molecules for improving the wound healing process. *European Journal of Pharmaceutics and Biopharmaceutics : Official Journal of Arbeitsgemeinschaft Fur Pharmazeutische Verfahrenstechnik e.V.*, 139, 1–22.
- Mistry, P., Chhabra, R., Muke, S., Narvekar, A., Sathaye, S., Jain, R., & Dandekar, P. (2021). Fabrication and characterization of starch-TPU based nanofibers for wound healing applications. *Materials Science & Engineering. C, Materials for Biological Applications*, 119, 111316.
- Nicosia, A., Keppler, T., Müller, F. A., Vazquez, B., Ravegnani, F., Monticelli, P., & Belosi, F. (2016). Cellulose acetate nanofiber electrospun on nylon substrate as novel composite matrix for efficient, heat-resistant, air filters. *Chemical Engineering Sciences*, 153, 284–294. <https://doi.org/10.1016/j.ces.2016.07.017>
- Niculescu, O., Leca, M., Moldovan, Z., & Deselnicu, D. C. (2015). Obtaining and characterization of a product with antifungal properties based on essential oils and natural waxes for finishing natural leathers. *Revista de Chimie-Bucharest*, 66(11), 157–163.
- Omollo, E., Zhang, C., Mwasiagi, J. I., & Ncube, S. (2016). Electrospinning cellulose acetate nanofibers and a study of their possible use in high-efficiency filtration. *Journal of Industrial Textiles*, 45(5), 716–729. <https://doi.org/10.1177/1528083714540696>
- Özgüney, I., Shuwisikül, D., & Bodmeier, R. (2009). Development and characterization of extended release Kollidon® SR mini-matrices prepared by hot-melt extrusion. *European Journal of Pharmaceutics and Biopharmaceutics : Official Journal of Arbeitsgemeinschaft Fur Pharmazeutische Verfahrenstechnik e.V.*, 73(1), 140–145. <https://doi.org/10.1016/j.ejpb.2009.04.006>
- Ramakrishna, S., Fujihara, K., Teo, W. E., Lim, T. C., & Ma, Z. (2005). *An introduction to electrospinning and nanofibers* (pp. 90–130). World Scientific.
- Rath, G., Hussain, T., Chauhan, G., Garg, T., & Goyal, A. K. (2016). Collagen nanofiber containing silver nanoparticles for improved wound-healing applications. *Journal of Drug Targeting*, 24(6), 520–529.
- Rho, K. S., Jeong, L., Lee, G., Seo, B. M., Park, Y. J., Hong, S. D., Roh, S., Cho, J. J., Park, W. H., & Min, B. M. (2006). Electrospinning of collagen nanofibers: Effects on the behavior of normal human keratinocytes and early-stage wound healing. *Biomaterials*, 27(8), 1452–1461. <https://doi.org/10.1016/j.biomaterials.2005.08.004>
- Sagiri, S. S., Behera, B., Pal, K., & Basak, P. (2013). Lanolin-based organogels as a matrix for topical drug delivery. *Journal of Applied Polymer Science*, 128(6), 3831–3839. <https://doi.org/10.1002/app.38590>
- Samimi Gharai, S., Habibi, S., & Nazockdast, H. (2018). Fabrication and characterization of chitosan/gelatin/thermoplastic polyurethane blend nanofibers. *Journal of Textiles and Fibrous Materials*, 1, 2515221118769324.
- Sasaki, B. C., Pinkerton, K., & Leipelt, A. (2014). Does lanolin use increase the risk for infection in breastfeeding women? *Clinical Lactation*, 5(1), 28–32. <https://doi.org/10.1891/2158-0782.5.1.28>
- Shi, Y., Wei, Z., Zhao, H., Liu, T., Dong, A., & Zhang, J. (2013). Electrospinning of ibuprofen-loaded composite nanofibers for improving the performances of transdermal patches. *Journal of Nanoscience and Nanotechnology*, 13(6), 3855–3863. <https://doi.org/10.1166/jnn.2013.7157>
- Silva, C. L., Pereira, J. C., Ramalho, A., Pais, A. A., & Sousa, J. J. (2008). Films based on chitosan polyelectrolyte complexes for skin drug delivery: Development and characterization. *Journal of Membrane Science*, 320(1–2), 268–279. <https://doi.org/10.1016/j.memsci.2008.04.011>
- Sofi, H. S., Akram, T., Tamboli, A. H., Majeed, A., Shabir, N., & Sheikh, F. A. (2019). Novel lavender oil and silver nanoparticles simultaneously loaded onto polyurethane nanofibers for wound-healing applications. *International Journal of Pharmaceutics*, 569, 118590.
- Stanger, J., Tucker, N., & Staiger, M. (2005). Electrospinning. *Rapra Review Reports*, 16(10), 218.
- Taepaiboon, P., Rungsardthong, U., & Supaphol, P. (2006). Drug-loaded electrospun mats of poly (vinyl alcohol) fibres and their release characteristics of four model drugs. *Nanotechnology*, 17(9), 2317–2329. <https://doi.org/10.1088/0957-4484/17/9/041>
- Taepaiboon, P., Rungsardthong, U., & Supaphol, P. (2007). Vitamin-loaded electrospun cellulose acetate nanofiber mats as transdermal and dermal therapeutic agents of vitamin A acid and vitamin E. *European Journal of Pharmaceutics and Biopharmaceutics : Official Journal of Arbeitsgemeinschaft Fur Pharmazeutische Verfahrenstechnik e.V.*, 67(2), 387–397.
- Tait, P. (2000). Nipple pain in breastfeeding women: Causes, treatment, and prevention strategies. *Journal of Midwifery & Women's Health*, 45(3), 212–215. [https://doi.org/10.1016/S1526-9523\(00\)00011-8](https://doi.org/10.1016/S1526-9523(00)00011-8)
- Tanzi, M. C., Mantovani, D., Petrini, P., Guidoin, R., & Laroche, G. (1997). Chemical stability of polyether urethanes versus polycarbonate urethanes. *Journal of Biomedical Materials Research*, 36(4), 550–559. [https://doi.org/10.1002/\(SICI\)1097-4636\(19970915\)36:4<550::AID-JBM14>3.0.CO;2-E](https://doi.org/10.1002/(SICI)1097-4636(19970915)36:4<550::AID-JBM14>3.0.CO;2-E)
- Topuz, F., Abdulhamid, M. A., Holtzl, T., & Szekeley, G. (2021). Nanofiber engineering of microporous polyimides through electrospinning: Influence of electrospinning parameters and salt addition. *Materials & Design*, 198, 109280. <https://doi.org/10.1016/j.matdes.2020.109280>
- Tungprapa, S., Jangchud, I., & Supaphol, P. (2007). Release characteristics of four model drugs from drug-loaded electrospun cellulose acetate fiber mats. *Polymer*, 48(17), 5030–5041. <https://doi.org/10.1016/j.polymer.2007.06.061>
- Wilhelm, C., Rivaton, A., & Gardette, J. L. (1998). Infrared analysis of the photochemical behaviour of segmented polyurethanes: 3. Aromatic diisocyanate based polymers. *Polymer*, 39(5), 1223–1232. [https://doi.org/10.1016/S0032-3861\(97\)00353-4](https://doi.org/10.1016/S0032-3861(97)00353-4)
- Xu, X., Jiang, L., Zhou, Z., Wu, X., & Wang, Y. (2012). Preparation and properties of electrospun soy protein isolate/polyethylene oxide nanofiber membranes. *ACS Applied Materials & Interfaces*, 4(8), 4331–4337. <https://doi.org/10.1021/am300991e>
- Yılmaz, E., Uslu, E. K., & Toksöz, B. (2020). Structure, rheological and sensory properties of some animal wax based oleogels. *Journal of Oleo Science*, 69(10), 1317–1329.
- Yong, L., Jia, L., Jie, F., & Meng, W. (2014). Preparation and characterization of electrospun human hair keratin/poly (ethylene oxide) composite nanofibers. *Matéria (Rio de Janeiro)*, 19(4), 382–388. <https://doi.org/10.1590/S1517-70762014000400009>
- Zarghami, A., Irani, M., Mostafazadeh, A., Golpour, M., Heidarinasab, A., & Haririan, I. (2015). Fabrication of PEO/chitosan/PCL/olive oil nanofibrous scaffolds for wound dressing applications. *Fibers and Polymers*, 16(6), 1201–1212. <https://doi.org/10.1007/s12221-015-1201-8>
- Zdrachala, R. J., & Zdrachala, I. J. (1999). Biomedical applications of polyurethanes: A review of past promises, present realities, and a vibrant future. *Journal of Biomaterials Applications*, 14(1), 67–90. <https://doi.org/10.1177/088532829901400104>
- Zhang, K., Bai, X., Yuan, Z., Cao, X., Jiao, X., Li, Y., Qin, Y., Wen, Y., & Zhang, X. (2019). Layered nanofiber sponge with an improved capacity for promoting blood coagulation and wound healing. *Biomaterials*, 204, 70–79.
- Zhou, W., He, J., Cui, S., & Gao, W. (2011). Studies of electrospun cellulose acetate nanofibrous membranes. *The Open Materials Science Journal*, 5(1), 51–55.